

PAPER • OPEN ACCESS

Gallium vacancies—common non-radiative defects in ternary GaAsP and quaternary GaNAsP nanowires

To cite this article: J E Stehr *et al* 2020 *Nano Ex.* 1 020022

View the [article online](#) for updates and enhancements.



PAPER

Gallium vacancies—common non-radiative defects in ternary GaAsP and quaternary GaNAsP nanowires

OPEN ACCESS

RECEIVED
5 May 2020REVISED
11 July 2020ACCEPTED FOR PUBLICATION
21 July 2020PUBLISHED
11 August 2020

Original content from this work may be used under the terms of the [Creative Commons Attribution 4.0 licence](#).

Any further distribution of this work must maintain attribution to the author(s) and the title of the work, journal citation and DOI.

J E Stehr^{1,3} , M Jansson¹ , R La², C W Tu², W M Chen¹ and I A Buyanova^{1,3} ¹ Department of Physics, Chemistry and Biology, Linköping University, 581 83 Linköping, Sweden² Department of Electrical and Computer Engineering, University of California San Diego, La Jolla, California 92093, United States of America³ Authors to whom any correspondence should be addressed.E-mail: jan.eric.stehr@liu.se and irina.bouianova@liu.se**Keywords:** nanowires, GaNAsP, defects, ODMR, photoluminescenceSupplementary material for this article is available [online](#)**Abstract**

Nanowires (NWs) based on ternary GaAsP and quaternary GaNAsP alloys are considered as very promising materials for optoelectronic applications, including in multi-junction and intermediate band solar cells. The efficiency of such devices is expected to be largely controlled by grown-in defects. In this work we use the optically detected magnetic resonance (ODMR) technique combined with photoluminescence measurements to investigate the origin of point defects in Ga(N)AsP NWs grown by molecular beam epitaxy on Si substrates. We identify gallium vacancies, which act as non-radiative recombination centers, as common defects in ternary and quaternary Ga(N)AsP NWs. Furthermore, we show that the presence of N is not strictly necessary for, but promotes, the formation of gallium vacancies in these NWs.

1. Introduction

Recently, group III–V nanowires (NWs) have attracted a growing interest as building blocks for optoelectronic and photovoltaic applications [1–6]. Due to their one-dimensional geometry, the NWs can exhibit structural [7, 8], electrical [9] and photonic properties [10–13] that are different from and are often superior to their bulk and thin-film counterparts. For example, the absorptivity of NWs can be increased substantially by tuning the geometry of the array structures [11], which boosts efficiency of NW solar cells above that of planar devices and allows to reduce material consumption and costs. Moreover, due to relaxed lattice-match constraints, NWs can be easily grown on foreign substrates. As a result, III–V NWs with superior optical properties can be integrated into mature Si-based electronic architectures.

Among III–V compounds and related alloys, GaAsP is of particular interest. This is because the bandgap energy of this material can be tuned within the 1.4–2.3 eV range, attractive for using this alloy in multi-junction solar cells [5, 14, 15]. Further bandgap tunability can be achieved by alloying GaAsP with a few percent of N as a result of the giant bandgap bowing [16–18]. Moreover, an anticrossing interaction between the N localized states and the host states in dilute nitrides results in splitting of the conduction band into two sub-bands (E^+ and E^-) [19, 20]. This splitting can be utilized in novel intermediate-band solar cells [21], where the E^- states can be used as a stepping stone for two-step two-photon transitions enabling absorption of low-energy photons, in addition to the band-to-band absorption involving the E^+ states. The highest efficiency of these devices is predicted [22] when the total bandgap energy is 1.95 eV, making GaNAsP attractive for applications in not only multi-junction but also intermediate-band solar cells [16, 17].

The efficiency of solar cells, as well as other optoelectronic devices, is strongly affected by non-radiative recombination (NRR), which introduces an additional loss of photo-created carriers and deteriorates extraction efficiency of the photo-generated carriers. In GaAs(P)- and InP-based NWs, the commonly discussed causes of NRR centers include structural defects [9, 23–27], such as twin boundaries and stacking faults, as well as surface

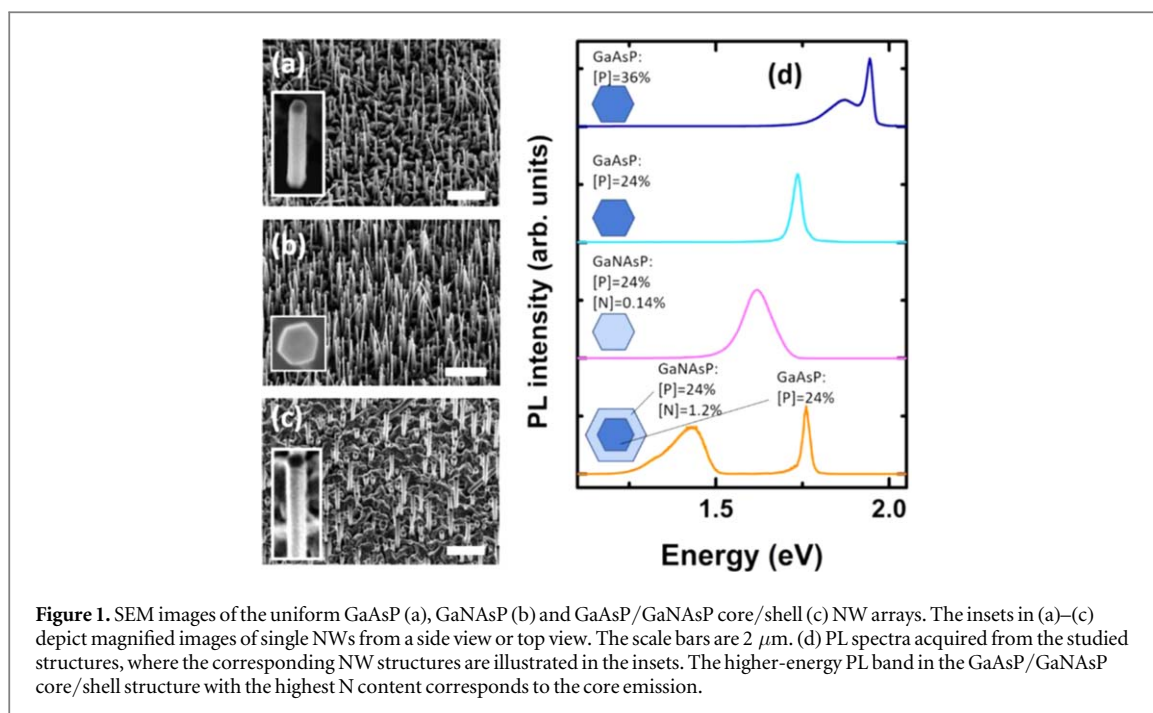


Figure 1. SEM images of the uniform GaAsP (a), GaNAsP (b) and GaAsP/GaNAsP core/shell (c) NW arrays. The insets in (a)–(c) depict magnified images of single NWs from a side view or top view. The scale bars are $2\ \mu\text{m}$. (d) PL spectra acquired from the studied structures, where the corresponding NW structures are illustrated in the insets. The higher-energy PL band in the GaAsP/GaNAsP core/shell structure with the highest N content corresponds to the core emission.

Table 1. Average dimensions of the investigated NWs determined by SEM.

| | Diameter (nm) | Length (μm) |
|--------------|---------------|--------------------------|
| GaAsP NWs | 70 | 2.4 |
| GaNAsP NWs | 120 | 1.7 |
| GaAsP/GaNAsP | 250 (total) | 1.7 |
| c/s NWs | 70 (core) | |

states [5, 28] that become significant because of a large surface-to-volume ratio. Recently we have shown [29–31] that NRR processes in NWs can also be related to the presence of point defects that are formed in bulk regions of the NWs, unrelated to the surface. Such defects will likely control NRR processes in optimized NW structures that are free from structural defects and have a passivated surface. Though NRR via point defects was also suggested in Ga(N)AsP NWs [26], their chemical origin remains unknown. In this work we investigate the origin of point defects in Ga(N)AsP NWs and their role in carrier recombination by using the optically detected magnetic resonance (ODMR) technique in combination with photoluminescence (PL) measurements.

2. Methods

The investigated NW arrays were grown on (111) Si substrates by using Ga-droplet catalyzed gas-source molecular beam epitaxy (MBE). The investigated structures include: (i) uniform GaAsP NWs with P compositions [P] of 24% and 36%; (ii) uniform GaNAsP NWs with [N] = 0.14% and [P] = 24%; and (iii) GaAsP/GaNAsP core/shell NW structures with [N] = 1.2% and [P] = 24%. The growth of the uniform NWs and the GaAsP core in the core/shell structures was performed via the vapor-liquid-solid mode at $620\ ^\circ\text{C}$ and $590\ ^\circ\text{C}$, respectively, whereas the growth temperature was lowered down to $500\ ^\circ\text{C}$ during the vapor-solid growth of the GaNAsP shell. The V/III incorporation ratio during the NW growth was 2. Using the core/shell design was required to increase the nitrogen content in GaNAsP. Full details on the growth conditions can be found in [32]. Typical scanning electron microscopy (SEM) images of the fabricated GaAsP, GaNAsP and GaAsP/GaNAsP NW arrays are shown in figures 1(a)–(c), respectively. Information on the dimensions of the NWs can be found in table 1. Apparently, a majority of the NWs are oriented along the direction normal to the substrate surface, i.e. following the Si [111] crystal orientation. Some of them, however, are randomly tilted from the [111] direction by up to 20° and a few NWs were toppled over. This distribution in the NW orientation was taken into account in the analysis of the ODMR signals using the Easyspin software package [33].

The PL spectra were acquired at 4 K, using a cw 532-nm solid state laser for excitation and a Si charged-coupled device (CCD) attached to a single grating monochromator for detection. The ODMR measurements

were performed at 4 K at microwave frequencies of ~ 9.4 GHz (X-band) and ~ 34 GHz (Q-band) with adjustable microwave powers. The 532-nm solid-state laser or a tunable Ti:sapphire cw laser operating at 740 nm were used as excitation sources. The ODMR signals were detected using a Si detector as microwave-induced changes of the PL intensity within the spectral range of 650–1000 nm. By using this spectral range, which is beyond the spectral range of light emissions from Si, we can safely exclude any possible contribution from the substrate to the detected ODMR signals.

3. Results and discussion

Figure 1(d) demonstrates changes in the near-band-edge PL emission from the investigated NWs upon P and N incorporation. According to our previous studies [18], the detected emission is dominated by recombination of localized excitons formed by long-range alloy fluctuations and its high energy cut-off corresponds to the alloy bandgap (E_g). The weak low-energy PL band in the GaAsP NWs with [P] = 36% is likely related to a defect/residual contaminant of unknown origin. Decreasing the P content in the ternary GaAsP structures from 36% (the dark blue curve) to 24% (the light blue curve) leads to the expected redshift of the emission photon energy. Introducing nitrogen in the alloy, while keeping the P content constant at 24%, further drastically reduces the bandgap of the NWs due to the giant bandgap bowing effect common for dilute nitride alloys [34]. In the alloy with 1.2% N (the orange curve) the bandgap shifts to 1.5 eV, i.e. by more than 300 meV from E_g of the parental GaAsP (~ 1.8 eV), highlighting the high tunability of the bandgap in dilute nitrides. The PL broadening in the N-containing NWs is caused by fluctuations in the N content, which translates in large changes of the bandgap energy due the giant bowing effect. Increasing measurement temperature caused a significant decrease in the PL intensity (by about 3 orders of magnitude between 4 K and 300 K), indicative for strong NRR in the studied NWs.

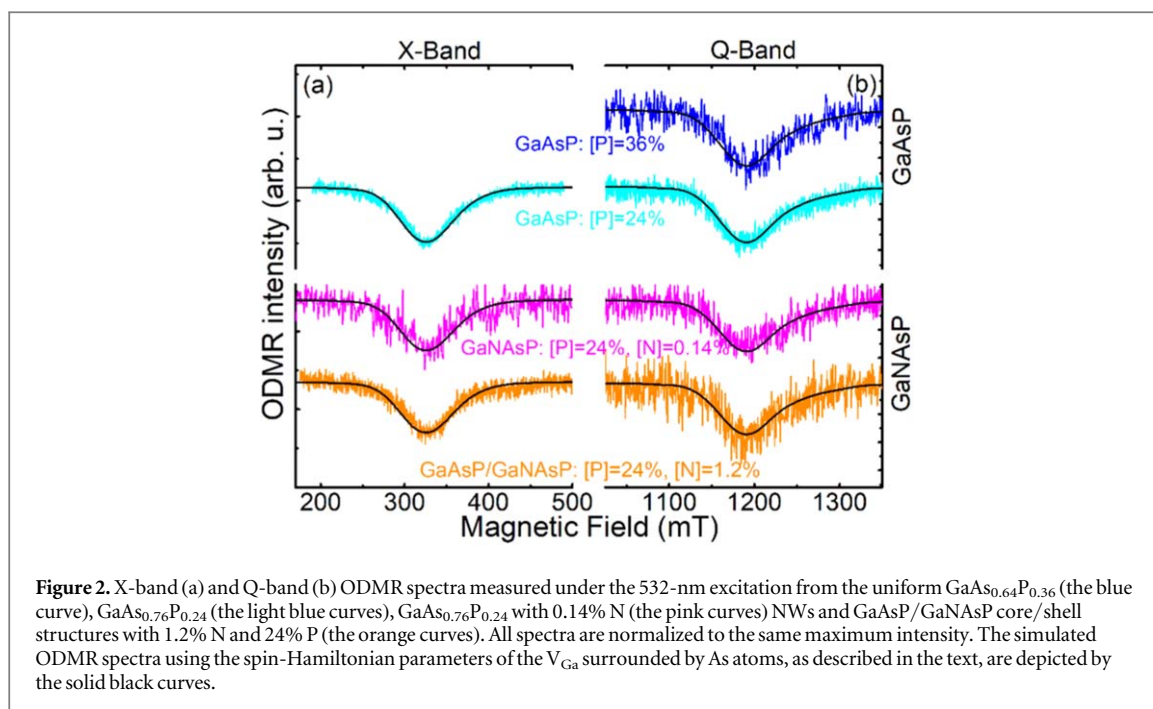
To gain an understanding on how the As/P ratio and alloying with N affects the formation of point defects responsible for NRR and to single out their possible chemical origin, we performed ODMR experiments. This technique not only provides chemical identity of the defects but also allows to single out their role in carrier recombination processes [35]. The ODMR spectra were analyzed by using the following spin Hamiltonian:

$$\mathcal{H} = \mu_B \mathbf{B} \mathbf{g} \mathbf{S} + \mathbf{S} \mathbf{A} \mathbf{I} \quad (1)$$

Here μ_B is the Bohr magneton, \mathbf{B} is an external magnetic field, \mathbf{S} represents the effective electron spin operator, \mathbf{I} the effective nuclear spin operator and \mathbf{g} and \mathbf{A} denote the electron g-tensor and hyperfine (hf) tensor, respectively. The Zeeman interaction is described by the first term in equation (1), while the second term describes the hyperfine interaction.

Figure 2 depicts the ODMR signals of the same NWs as shown in figure 1. All the ODMR spectra contain a broad signal displaying a negative intensity, which means that accelerated recombination via defects under magnetic resonance conditions leads to a decrease of the monitored near-band-edge emission by reducing a number of photo-generated carriers available for recombination processes. This, in turn, provides the evidence that the involved defects are involved in a recombination process that competes with the monitored radiative recombination, i.e. acts as NRR centers [35]. Following equation (1), the broadening of the ODMR spectra could be caused by two reasons. The first possibility is that it reflects contributions of several overlapping signals stemming from different defects with an electron spin of $S = 1/2$, but slightly different g-values (as described by the first term in equation (1)). Alternatively, it may be caused by the hyperfine interaction between the electron and nuclear spins of the same defect (represented by the second term in equation (1)). To distinguish which possibility is the cause of the ODMR signal broadening, we performed ODMR experiments at different microwave frequencies keeping in mind that the broadening induced by different defects with different g-factors should scale with the microwave frequency whereas the hf-induced broadening does not. These experiments revealed that the spectra measured at both X- and Q-band exhibit the same linewidth and signal shape (the solid colored curves in figures 2(a) and (b)), proving that the broadening of the ODMR signal is determined by the hf interaction. From the best fit to the experimental data, the following spin Hamiltonian parameters can be obtained: $S = 1/2$, $I = 3/2$, $g_{\parallel} = 1.98$, $g_{\perp} = 2.08$, $A_{\parallel} = 280 \times 10^{-4} \text{ cm}^{-1}$ and $A_{\perp} = 130 \times 10^{-4} \text{ cm}^{-1}$. The analysis can also satisfactorily describe the measured angular dependences of the ODMR signal. (The parallel and perpendicular orientations are given with respect to the crystallographic [111] axis). The simulated ODMR spectra using these parameters are shown by the solid black curves in figure 2. In the simulations, we considered random orientations of some of the NWs with tilting angles up to 20° from the vertical [111] direction, as revealed by SEM shown in figures 1(a) and (b). This was done by averaging the simulated ODMR spectra over all possible NW orientations, which resulted in broadening and merging of the ODMR signals.

Judging from the deduced spin-Hamiltonian parameters, the signal can be assigned to a gallium vacancy (V_{Ga}) with a hyperfine interaction between an unpaired electron spin $S = 1/2$ and an ^{75}As nucleus with a nuclear spin $I = 3/2$ and 100% natural abundance, stemming from the Ga vacancy having neighboring As atoms. This

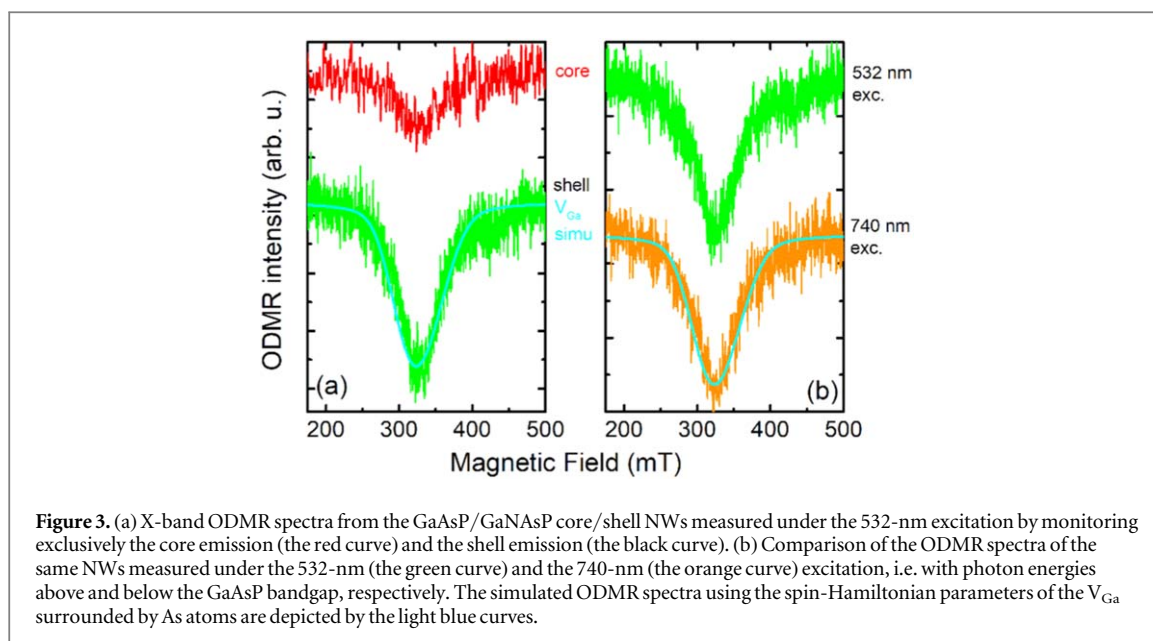


defect was observed previously in electron irradiated GaAs bulk crystals [36] and GaNAs NWs [29, 30]. It is interesting to note that in the studied NWs with [P] up to 36% the closest neighbors of the defect could include P and/or As atoms. However, the measured ODMR spectra can only be simulated assuming that the detected V_{Ga} have only As atoms in its immediate surrounding. This is because the spin-Hamiltonian parameters of the defect are known to be very sensitive to its local structure. For example, if the V_{Ga} would be solely surrounded by P atoms instead of As atoms, the g-value would be isotropic with $g = 2.016$ (see the supporting information is available online at stacks.iop.org/NANOX/1/020022/mmedia for more details) [37]. Since within the experimental accuracy we cannot observe the ODMR signal of V_{Ga} surrounded by P atoms, i.e. it must be at least 20 times weaker than the ODMR signal of V_{Ga} surrounded by As (see supporting information), we can conclude that the formation of gallium vacancies is favorable under As-rich local surrounding, in spite of the considerable P content in the alloys. Moreover, the defect should reside in the volume region of the nanowire, as a defect close to the surface would otherwise lead to a significant re-distribution of electron wavefunction and, thus, modifications of the spin-Hamiltonian parameters.

We shall now determine if the presence of N in the NWs influences the formation of the V_{Ga} center. Figure 3(a) depicts ODMR spectra from the GaNAsP core/shell NWs with 1.2% N and 24% P content by monitoring exclusively the PL band from the core emission (the red curve) and the shell emission (the black curve).

The spectra were measured under laser excitation at 540 nm, i.e. under the conditions when all regions of the structure can be excited. It is obvious that the intensity of the ODMR signal is significantly higher when detecting the GaNAsP emission, which suggests that the concentration of the Ga vacancies is substantially higher in GaNAsP. To confirm this result, we performed additional ODMR experiments under laser excitation at 740 nm, which only selectively excited the GaNAsP shell with the bandgap of 1.5 eV but not the GaAsP core. The observation of the same ODMR signal under such conditions, see figure 3(b), provides a further proof that the V_{Ga} ODMR signal predominantly stems from the GaNAsP shell. The obtained result suggests that the formation of the gallium vacancies is promoted by the presence of N, though the lower growth temperature used during the growth of the GaNAsP shell could also somewhat enhance the defect formation. This is consistent with the previous experimental studies reporting an enhanced V_{Ga} formation upon alloying with N in GaNAs NWs [28] and GaNAs [38, 39] epilayers, as well as with the results of first-principles calculations, which have concluded that the formation of V_{Ga} becomes more energetically favorable in the presence of N [40].

It is interesting to note that in the past gallium vacancies in bulk and thin films of GaAs and GaP were mainly detected either after irradiation by energetic particles [36, 37, 41, 42] or in highly-doped n-type materials [43]. In undoped planar structures, the defect formation was found to be significantly enhanced in the presence of nitrogen in dilute III-N-V alloys [38–40]. Our results show that even though N incorporation promotes the V_{Ga} formation in the NW structures, the defects also readily form in N-free GaAsP and GaAs [30] grown by MBE. This can be attributed to different growth conditions of the NWs as compared to bulk and thin films. Similar



behavior was also observed in ZnO where certain defects were found to be exclusively formed in NWs but not in bulk or thin films [31].

4. Conclusion

In summary, we have employed PL and ODMR spectroscopies to study defect formation in the MBE-grown Ga(N)AsP NWs. Gallium vacancies are found to be the common grown-in defects in the NWs grown in both vapor-liquid-solid and vapor-solid modes. Based on the similarity of the deduced spin-Hamiltonian parameters with the known parameters of V_{Ga} in bulk GaAs, the defect is concluded to be formed in volume regions of the NW and is favored under As-rich local surrounding. It acts as an efficient NRR center competing with radiative recombination in the alloys. Our finding, therefore, calls for future efforts in developing strategies to suppress the defect formation during the growth, crucial for applications of Ga(N)AsP NWs in novel optoelectronic devices.

Acknowledgments

The authors are grateful for the financial support by Linköping University through the Professor Contracts and the Swedish Research Council (Grant No. 2019-04312). IB and WC acknowledge the financial support by Swedish Government Strategic Research Area in Materials Science on Functional Materials at Linköping University (Faculty Grant SFO-Mat-LiU No 2009 00971).

ORCID iDs

J E Stehr <https://orcid.org/0000-0001-7640-8086>
 M Jansson <https://orcid.org/0000-0001-5751-6225>
 W M Chen <https://orcid.org/0000-0002-6405-9509>
 I A Buyanova <https://orcid.org/0000-0001-7155-7103>

References

- [1] Gudiksen M S, Lauhon L J, Wang J, Smith D C and Lieber C M 2002 Growth of nanowire superlattice structures for nanoscale photonics and electronics *Nature* **415** 617
- [2] Li Y, Qian F, Xiang J and Lieber C M 2006 Nanowire electronic and optoelectronic devices *Mater. Today* **9** 18–27
- [3] Yan R, Gargas D and Yang P 2009 Nanowire photonics *Nat. Photonics* **3** 569–76
- [4] Joyce H J *et al* 2011 III–V semiconductor nanowires for optoelectronic device applications *Progr. Quantum Electron.* **35** 23–75
- [5] Holm J V, Krogstrup P, Liu H and Aagesen M 2013 Surface-passivated GaAsP single-nanowire solar cells exceeding 10% efficiency grown on silicon *Nat. Commun.* **4** 1498
- [6] Eaton S W, Fu A, Wong A B, Ning C and Yang P 2016 Semiconductor nanowire lasers *Nat. Rev. Mater.* **1** 16028

- [7] Caroff P, Johansson J, Messing M E, Deppert K and Samuelson L 2009 Controlled polytypic and twin-plane superlattices in III–V nanowires *Nat. Nanotechnol.* **4** 50–5
- [8] Assali S et al 2013 Direct band gap wurtzite gallium phosphide nanowires *Nano Lett.* **13** 1559–63
- [9] Parkinson P, Joyce H J, Gao Q, Tan H H, Zhang X, Zou J, Jagadish C, Herz L M and Johnston M B 2009 Carrier lifetime and mobility enhancement in nearly defect-free core–shell nanowires measured using time-resolved terahertz spectroscopy *Nano Lett.* **9** 3349–53
- [10] Sirbuly D J, Tao A, Law M, Fan R and Yang P 2007 Multifunctional nanowire evanescent wave optical sensors *Adv. Mater.* **19** 61–6
- [11] Wallentin J et al 2013 InP nanowire array solar cells achieving 13.8% efficiency by exceeding the ray optics limit *Science* **339** 1057–60
- [12] Saxena D, Mokkalapati S, Parkinson P, Jiang N, Gao Q, Tan H H and Jagadish C 2013 Optically pumped room-temperature GaAs nanowire lasers *Nat. Photonics* **7** 963–8
- [13] Chen S, Jansson M, Stehr J E, Huang Y, Ishikawa F, Chen W M and Buyanova I A 2017 Dilute nitride nanowire lasers based on a GaAs/GaNAs core/shell structure *Nano Lett.* **17** 1775–81
- [14] Lapiere R R 2011 Theoretical conversion efficiency of a two-junction III–V nanowire on Si solar cell *J. Appl. Phys.* **110** 014310
- [15] Vaisman M, Fan S, Yaung K N, Perl E, Martín-Martín D, Yu Z J, Leilaouiou M, Holman Z C and Lee M L 2017 15.3%-efficient GaAsP solar cells on GaP/Si templates *ACS Energy Lett.* **2** 1911–8
- [16] Kuang Y J, Yu K M, Kudrawiec R, Luce A V, Ting M, Walukiewicz W and Tu C W 2013 GaNAsP: an intermediate band semiconductor grown by gas-source molecular beam epitaxy *Appl. Phys. Lett.* **102** 112105
- [17] Kudrawiec R, Luce A V, Gladysiewicz M, Ting M, Kuang Y J, Tu C W, Dubon O D, Yu K M and Walukiewicz W 2014 Electronic band structure of GaN_xPyAs_{1-x-y} highly mismatched alloys: suitability for intermediate-band solar cells *Phys. Rev. Appl.* **1** 0034007
- [18] Jansson M, Chen S, La R, Stehr J E, Tu C W, Chen W M and Buyanova I A 2017 Effects of nitrogen incorporation on structural and optical properties of GaNAsP nanowires *J. Phys. Chem. C* **121** 7047–55
- [19] Perkins J D, Mascarenhas A, Zhang Y, Geisz J F, Friedman D J, Olson J M and Kurtz S R 1999 Nitrogen-activated transitions, level repulsion, and band gap reduction in GaAs_{1-x}N_x with $x < 0.03$ *Phys. Rev. Lett.* **82** 3312–5
- [20] Shan W, Walukiewicz W, Ager J III, Haller E E, Geisz J F, Friedman D J, Olson J M and Kurtz S R 1999 Band anticrossing in GaInNAs alloys *Phys. Rev. Lett.* **82** 1221–4
- [21] López N, Reichertz L a, Yu K M, Campman K and Walukiewicz W 2011 Engineering the electronic band structure for multiband solar cells *Phys. Rev. Lett.* **106** 028701
- [22] Luque A, Martí A and Stanley C 2012 Understanding intermediate-band solar cells *Nat. Photonics* **6** 146–52
- [23] Dobrovolsky A, Persson P O Å, Sukriattanon S, Kuang Y, Tu C W, Chen W M and Buyanova I A 2015 Effects of polytypism on optical properties and band structure of individual Ga(N)P nanowires from correlative spatially resolved structural and optical studies *Nano Lett.* **15** 4052
- [24] Sanchez A M, Zhang Y, Tait E W, Hine N D M, Liu H and Beanland R 2017 Nonradiative step facets in semiconductor nanowires *Nano Lett.* **17** 2454–9
- [25] Himwas C, Collin S, Rale P, Chauvin N, Patriarche G, Oehler F, Julien F H, Travers L, Harmand J C and Tchernycheva M 2017 *In situ* passivation of GaAsP nanowires *Nanotechnology* **28** 495707
- [26] Jansson M, Francaviglia L, La R, Balagula R, Stehr J E, Tu C W, Fontcuberta i Morral A, Chen W M and Buyanova I A 2019 Increasing N content in GaNAsP nanowires suppresses the impact of polytypism on luminescence *Nanotechnology* **30** 405703
- [27] Woo R L, Xiao R, Kobayashi Y, Gao L, Goel N, Hudait M K, Mallouk T E and Hicks R F 2008 Effect of twinning on the photoluminescence and photoelectrochemical properties of indium phosphide nanowires grown on silicon (111) *Nano Lett.* **8** 4664–9
- [28] Mohseni P K, Rodrigues A D, Galzerani J C, Pusep Y A and LaPierre R R 2009 Structural and optical analysis of GaAsP/GaP core–shell nanowires *J. Appl. Phys.* **106** 124306
- [29] Stehr J E, Chen S L, Jansson M, Ishikawa F, Chen W M and Buyanova I A 2016 Defect formation in GaAs/GaN_xAs_{1-x} core/shell nanowires *Appl. Phys. Lett.* **109** 203103
- [30] Stehr J E, Balagula R M, Jansson M, Yukimune M, Fujiwara R, Ishikawa F, Chen W M and Buyanova I A 2020 Effects of growth temperature and thermal annealing on optical quality of GaNAs nanowires emitting in the near-infrared spectral range *Nanotechnology* **31** 065702
- [31] Stehr J E, Chen S L, Chen W M, Cai L, Shen S and Buyanova I A 2019 Identification of a nitrogen-related acceptor in ZnO nanowires *Nanoscale* **11** 10921–6
- [32] La R, Pan J L, Bastiman F and Tu C W 2016 Self-catalyzed Ga(N)AsP nanowires and GaAsP/GaNAsP core–shell nanowires grown on Si (111) by gas-source molecular beam epitaxy *J. Vac. Sci. Technol. B, Nanotechnol. Microelectron. Mater. Process. Meas. Phenom.* **34** 02L108
- [33] Stoll S and Schweiger A 2006 EasySpin, a comprehensive software package for spectral simulation and analysis in EPR *J. Magn. Reson.* **178** 42–55
- [34] Buyanova I A and Chen W M 2019 Dilute nitrides-based nanowires—a promising platform for nanoscale photonics and energy technology *Nanotechnology* **30** 292002
- [35] Chen W M 2000 Applications of optically detected magnetic resonance in semiconductor layered structures *Thin Solid Films* **364** 45–52
- [36] Jia Y Q, von Bardeleben H J, Stievenard D and Delerue C 1992 Electron-paramagnetic-resonance observation of gallium vacancy in electron-irradiated p-type GaAs *Phys. Rev. B* **45** 1645–9
- [37] Kennedy T A and Wilsey N D 1978 Identification of the isolated Ga vacancy in electron-irradiated GaP through EPR *Phys. Rev. Lett.* **41** 977–80
- [38] Li W, Pessa M, Ahlgren T and Decker J 2001 Origin of improved luminescence efficiency after annealing of Ga(In)NAs materials grown by molecular-beam epitaxy *Appl. Phys. Lett.* **79** 1094–6
- [39] Toivonen J, Hakkarainen T, Sopanen M, Lipsanen H, Oila J and Saarinen K 2003 Observation of defect complexes containing Ga vacancies in GaAsN *Appl. Phys. Lett.* **82** 40–2
- [40] Janotti A, Wei S H, Zhang S B, Kurtz S and Van de Walle C G 2003 Interactions between nitrogen, hydrogen, and gallium vacancies in (formula presented) alloys *Phys. Rev. B* **67** 161201
- [41] Goltzene A, Meyer B, Schwab C, Greenbaum S G, Wagner R J and Kennedy T A 1984 Electron paramagnetic resonance spectroscopy of fast neutron-generated defects in GaAs *J. Appl. Phys.* **56** 3394–8
- [42] Golzené A, Meyer B and Schwab C 1984 Experimental evidence for an associated defect model for the neutron generated AsGa center in gallium arsenide *Phys. Status Solidi* **123** K125–8
- [43] Laine T, Saarinen K, Mäkinen J, Hautojärvi P, Corbel C, Pfeiffer L and Citrin P 1996 Observation of compensating Ga vacancies in highly Si-doped GaAs *Phys. Rev. B* **54** R11050